DEVELOPMENT AND EVALUATION OF A C-1500 PICK-UP TRUCK MODEL FOR ROADSIDE HARDWARE IMPACT SIMULATION

Mr. Abdullatif K. Zaouk , Dr. Nabih E. Bedewi, Dr. Cing-Dao Kan, and Mr. Dhafer Marzougui

FHWA/NHTSA National Crash Analysis Center
The George Washington University

ABSTRACT

A detailed multi-purpose finite element model of a 1994 Chevrolet C-1500 pick-up truck was developed at the FHWA/NHTSA National Crash Analysis Center. The model is the first of its kind developed specifically to address vehicle safety issues, including front and side performance, as well as road side hardware design. In addition a reduced version of the C-1500 detailed model was developed as a "bullet" model to test various components of the detailed model.

These simulations are conducted in support of research studies undergoing at the National Highway Traffic Safety Administration (NHTSA) and the Federal Highway Administration (FHWA) to investigate vehicle compatibility, new offset barrier tests, and highway/vehicle safety issues. Full scale vehicle crash tests conducted by NHTSA and FHWA are used for evaluation of the performance of the model. Two tests are compared, a frontal impact with a full rigid wall and a corner impact to a 42-inch Vertical Concrete Median. The comparisons between tests and simulations in terms of overall impact deformation, component failure modes, velocity and acceleration at various locations in the vehicle are presented for both detailed and reduced models. Modeling issues including element size, connectivity, and slide line interface of different parts are discussed. In addition, some simulation related hardware and software issues are addressed.. Additional simulations need to be performed to fully evaluate and validate both detailed and reduced models.

INTRODUCTION

Finite element models of vehicles have been increasingly used in preliminary design analysis, component design, and vehicle crashworthiness evaluation, as well as roadside hardware design [3,4,5]. As these vehicle models are becoming more sophisticated over the years in terms of their accuracy, robustness, fidelity, and size, the need for developing multi-purpose models that can be used to address safety issues for a wide class of impact scenarios becomes more apparent[6,7,8,9,10,11].

Several vehicle models have been developed at the U. S. Department of Transportation over the past years. The number of elements ranges in size from five thousand elements based on the Ford Festiva to twenty nine thousand elements based on the Ford Taurus. Different frontal impact scenarios were exercised with these vehicles including rigid narrow objects, full and partial wall barriers, small sign supports and guardrail end terminals. However, the validity of these models in other impact scenarios remains questionable.

Today, with the availability of lower cost super computers based on Symmetric Multi-Processor (SMP) and Massively Parallel Processor (MPP) technologies, simulations of the aforementioned impact cases can be made more elaborate and efficient [12,13]. With these advancements, in the near future, a typical simulation conducted on an SMP or MPP can be performed on a workstation in a similar time. Meanwhile, with the projection that models will continue to grow in size based on the improvement in computation speed, research is needed to improve the modeling abilities and addition of detail and complexity. Furthermore, in order for the vehicle models to be useful for a wide range of impact conditions, the validation needs to be conducted for that whole range.

A detailed finite element model of the Chevrolet C-1500 pick-up was developed at NCAC for multi-purpose impact scenarios [14] .This model was evaluated for a frontal impact to a rigid barrier, as well as a corner impact into a New Jersey Shape Concrete Barrier [1] and a 42-inch Vertical Concrete Barrier [2]. The comparisons between tests and simulations in terms of overall impact deformation, component failure modes, velocity and acceleration at various locations in the vehicle shows good correlation. and consistency with the full scale tests.

The reduced model was developed at NCAC to evaluate various components of the detailed model, as well as for the analysis of roadside hardware. The overall goal for the reduced model was to be computationally effective, maximum CPU time of 3 hours on current high end workstations. To achieve that goal, the model size was limited to no more then 10,000 elements.

This paper describes the results of a non-linear finite element simulation of both detailed and reduced models. The comparison between the detailed and reduced models in terms of part geometry and mesh density is discussed. The comparisons between tests and simulations (detailed and reduced models) in terms of overall impact deformation, component failure modes, velocity and acceleration at various locations in the vehicle shows good correlation. and consistency with the full scale tests. Suggestion for further improvement in developing finite element vehicle models was also included.

MODEL DESCRIPTION

Truck Model and its LS-DYNA3D Input File

The finite element model of a 1994 Chevrolet C-1500 pick-up truck was developed at the NCAC for the Federal Highway Administration (FHWA) and the National Highway Traffic Safety Administration (NHTSA). The Chevrolet C-1500 truck is a multi-purpose pickup tuck. The vehicle obtained by the NCAC is a Regular- Cab, Fleetside Long-Box C-1500 with a total length of 5.4 meters (212.6 inches) and a wheelbase of 3.34 meters (131.5) inches. The engine is a 4.3 liter Vortec V6 with Electronic Fuel Injection coupled to a manual transmission with a rear wheel drive configuration. However, several other models exist, such as higher engine capacity, automatic transmission and four wheel drive configuration, with no change in the general geometry.

Detailed Truck Model

The truck was first disassembled and grouped into seven main groups, the frame, front inner, front outer, cabin, doors, bed and miscellaneous. The three dimensional geometric data of each component was then obtained by using a passive digitizing arm connected to a desktop computer. The surface patches generated from specified digitized data were stored in AutoCAD in IGES format. These IGES files were then imported into PATRAN [15] for mesh generation and model assembly. The model was then translated from PATRAN, which outputs a neutral file, into an LS-DYNA3D [16,17] input file using a translator called HPD [18] developed at the NCAC.

Since this model is used for multi-purpose crash applications, considerable detail was included in the rail frame, and front structures including bumper, radiator, radiator assembly, suspension, engine, side door and cabin of the vehicle. These parts were digitized as detailed as possible, minimizing any loss in the part’s geometry. For example, the chassis or main frame, one of the most important structural parts in the truck, was digitized and meshed using two different methods. The first did not include any of the buckling holes while the second included all these holes. In the first case, the model behaved poorly when compared to the test, however the second case behaved as expected. In including these holes, the running time increased. This was caused by the increase in element numbers and the decrease in the element size on the rails. However, there was a significant gain in the truck's behavior.

Another aspect of increasing the model's accuracy, is materials testing. Several coupons from parts such as the engine cradle, fender, hood, bumper, rails, door and door frame were tested to obtain their properties. Two types of tests were conducted on these parts, tension and shear. These tests were conducted at three different rates: slow static, low rate dynamic and high rate dynamic. The properties of these materials will be added to the model in the next phase of the truck model development.

As mentioned earlier, four LS-DYNA3D material models are used in the truck model. Table 1 lists the material model used along with the number of components. The first column corresponds to the material type number as used by LS-DYNA3D.

Table 1: LS-DYNA3D material models used for the detailed model

No.	**Material Type**	**No. of Components**
1	Elastic	25
7	Blatz-Ko Rubber	5
20	Rigid	27
24	Piecewise Linear Isotropic Plastic	154

The elastic material model (material type 1, table 2) was used in components such as the engine, transmission, mounts and radiator.

Table 2: Elastic material model

Elastic	
Density	7.85E-09 t/mm^3
Young's modulus	210,000 N/mm^2
Poisson's ratio	0.3

The Blatz-Ko material model (material type 7, table 3) was used in several mounts such as between the cabin and rails, engine and rails, etc.

Table 3: Blatz-Ko material model

Batz-Ko Rubber	
Density	0.95 t/mm^3
Young's modulus	28 N/mm^2

As seen from table 1, material type 24, the rate-dependent tabular isotropic elastic-plastic material model, is the most commonly used material type. Table 4 includes the values used for this material model in the truck simulation.

Table 4: Piecewise Linear Isotropic Plasticity material model

Piecewise Linear Isotropic Plasticity	
Density	7.85E-09 t/mm^3
Young's Modulus	210,000 N/mm^2
Poisson's Ratio	0.3
Yield Stress	215 N/mm^2
Load Curve	See figure 1
Plastic Strain at failure	∝ (no failure)

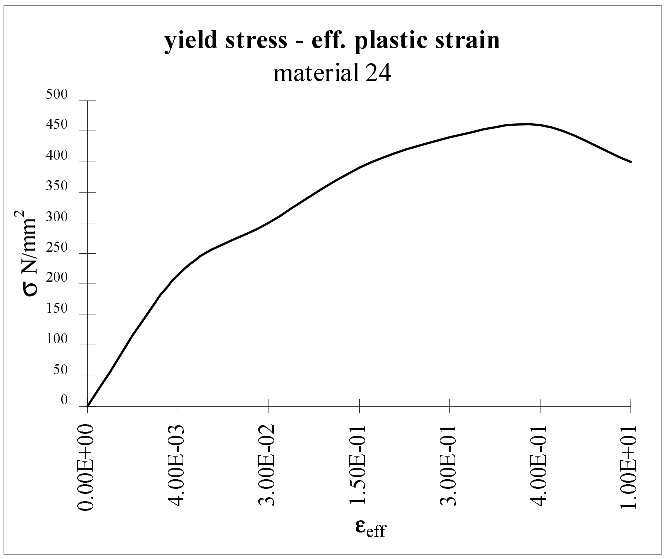

Figure 1: Load curve of yield stress vs. Effective plastic strain for material 24

In addition, to increase the accuracy of the model, each component is weighed and compared to the simulation weight. This comparison was limited to the accessible parts only. Table 5 lists the major components with the weight comparison between truck and FEM. It should be noted that each of these components is composed of several parts.

Table 5: Weight of various components

Component	**Actual Weight (Kg)**	**FEM Weight (kg)**
Door assembly	25.85	26.54

Bumper assembly	19.59	20.49
Fender	14.42	13.38
Hood	25.7	27.09
Radiator assembly	21.99	24.33

The center of gravity location (C.G.) of the model as taken from the truck model was then compared to the center of gravity location obtained from the 42-inch Vertical Concrete Barrier test. Table 6 shows the C.G. location comparison between test and FEM. The C.G. location of the FEM model is reasonable in comparison with the test, this confirms the accuracy of the geometry and weight distribution.

Table 6: Center of gravity location for the detailed model

	X (mm)	**Y (mm)**	**Z (mm)**
FEM	-2220.00	-19.75	803.00
Test	-2100.00	0.00	690.00

Parts are connected using three different types of connections: slidelines, constrained nodes, or joints. Slideline type-6, discrete node tied to a surface, was used if two close parallel elements needed to be tied together, such as in the case of the rails. Two types of nodal constraint, nodal rigid body constraint and spot weld, were used. Nodal rigid body constraint treats a group of nodes as one rigid body, the distance between these nodes is constant. However, these node can rotate in space. The second type of nodal constraint is the spot weld which can be treated as two nodes connected by a rigid beam. The nodes can move in space in translation and in rotation, but cannot translate or rotate relative to each other. Two types of joints, spherical and revolute, were used to connect the front suspension of the truck model. The contact between the different components of the vehicle was modeled using sliding interface Type-13 in LS-DYNA3D. In slideline type 13 only the slave materials are specified, and the orientation of the slideline segment is of no matter. These materials are checked against each other , and each material is checked against it self. Because the slideline check demands significant computational power, only the necessary components were included.

Figure 2 shows the isometric, top, and bottom views of the full C-1500 truck FE model, respectively. The hood of the truck was removed in the top view for display purposes.

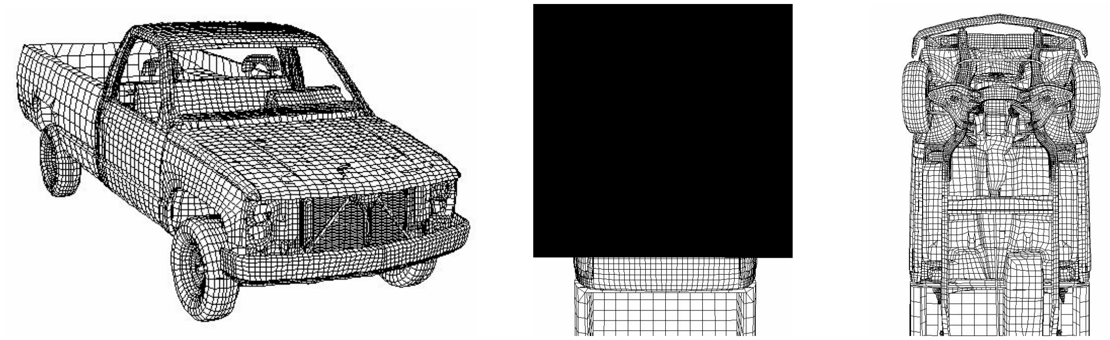

Figure 2: Isometric, top (no hood) and bottom views of the detailed truck model

Reduced Truck Model

The reduced truck model was created using the same IGES files generated for the full model. These IGES files were then imported into PATRAN [15] for mesh generation and model assembly. Large elements were used in the reduced model to reduce the total number of elements The new reduced model was then translated from a neutral file outputted from PATRAN into an LS-DYNA3D [16,17] input file using HPD [18], a PATRAN to LS-DYNA3D translator. Using large element size resulted in a considerable loss to the overall truck geometry. This is best illustrated in the rails, figure3, where the geometry changed from a c-channel type to a wide flanged c-channel. Figure 4 shows the difference between the reduced and full model geometry of the top and bottom A-Arms, apparent geometry losses can be seen at the corners where the small elements have been deleted.

Figure 3: Rails, detailed and reduced truck model respectively

Figure 4: Top and Bottom A-Arms of detailed and reduced truck model respectively

The reduced model consists of 9,745 nodes, 8,721 shell elements, 47 beam elements and 336 hexahedron elements. The PATRAN neutral file consists of 37 groups, corresponding to the number of element properties, as well as the number of all components. Specifically, the properties of each component are defined by a set of material cards with 3 types of materials being used in the model.

Each of the 39 components is subdivided into either shell elements, beam elements or hexahedron elements. The reduced model uses the same element formulation used in the full model.

As mentioned, three LS-DYNA3D material models are used in the reduced truck model. Table 7 lists the material models used along with the number of components. The first column corresponds to the material type number as used by LS-DYNA3D. The reduced model uses the same material models used by the full model (Tables 1,2 and 4). The Blatz-Ko material model was not used in the reduce model for simplicity and to reduce the computation time.

Table 7: LS-DYNA3D material models used for the reduced model

No.	Material Type	No. of Components
1	Elastic	9
20	Rigid	4
24	Piecewise Linear Isotropic Plastic	24

Similarly, the center of gravity location (C.G.) of the reduced model was compared to the center of gravity location obtained from the 42-inch Vertical Concrete Barrier test. Table 8 shows the C.G. location comparison between test and reduced truck model. The difference in the (x,y,z) location between the reduced model and the test could be attributed to the inaccuracies in the geometry, and to the number of parts included in the reduced model.

Table 8: Center of gravity location for the reduced model

	X (mm)	Y (mm)	Z (mm)
Reduced truck model	-1820.00	35.20	842.10
Test	-2100.00	0.00	690.00

Parts are connected using two different types of connections: constrained nodes, and merged nodes. As in the full model, two types of nodal constraint, group nodal constraint and spot weld, were used. Merging nodes is done by moving the nodes of the part to be connected contact entity option in LS-DYNA3D was used instead of the sliding interface type-13. New LS-DYNA3D input files for the truck to rigid full barrier and truck to 42-inch vertical barrier were generated and the initial velocities, simulation time step, and termination time were specified

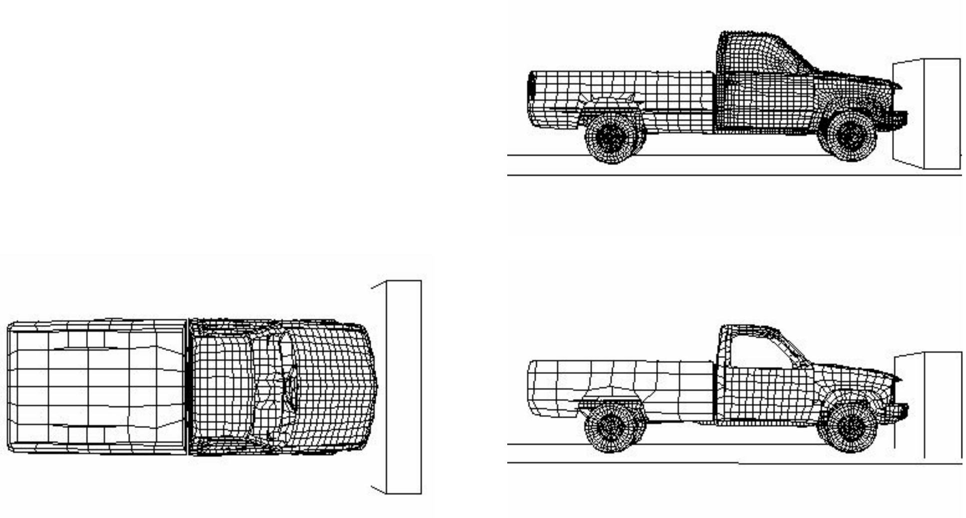

Figure 6: Frontal impact to a full rigid wall of detailed and reduced model

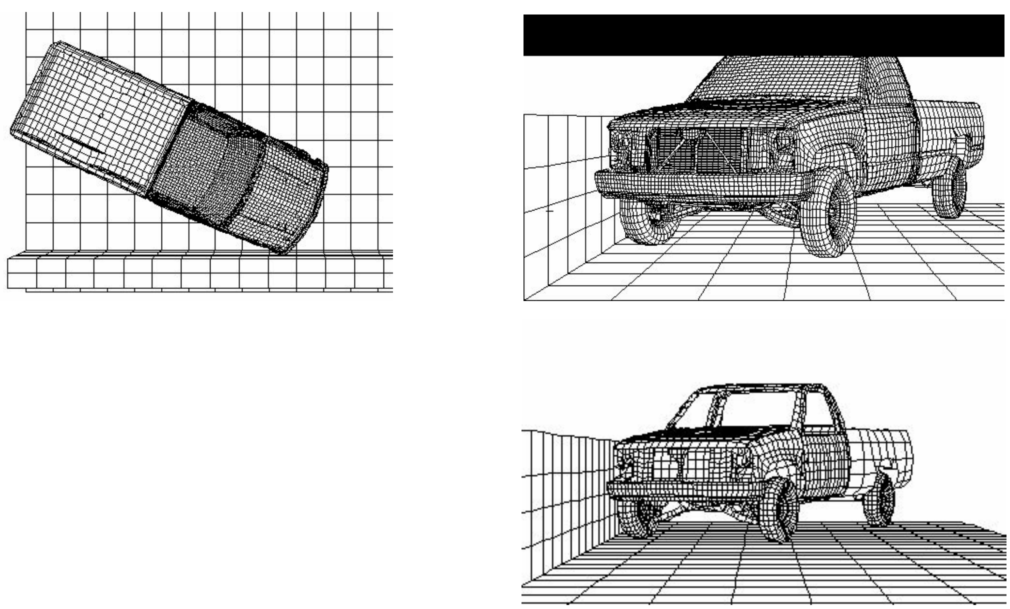

Figure 7: Corner impact to a 42 inch (1.07 m) concrete median of detailed and reduced model

TEST DESCRIPTION

The frontal impact of the C-1500 pick-up truck with a full rigid barrier was conducted as part of the New Car Assessment Program sponsored by NHTSA under Contract No. DTNH22-90-D-22121, while the corner impact with the 42 inch vertical barrier was conducted as part the National Cooperative Highway Research Program (NCHRP) by the FHWA under Contract No. DTFH61-95-C00136. The detail of the test vehicles and test impact conditions are listed in Tables 6 and 7. In test 1, several transducers were placed throughout the truck, including the engine, brake pad, dashboard, and seats. Data from these transducers are described in the next section along with the comparison to simulations.

Table 9: Description of Test 1

Test Number MN0111	
Test Date	July, 24, 1992
Test Configuration:	Vehicle into Frontal Rigid Barrier with 100% Overlap and 0 Degree Impact Angle
Vehicle:	Chevrolet C-1500 1992 Model Year;
Engine Type:	4.3 liter V6 transverse front mount
Transmission Type:	Automatic
Vehicle Speed:	56.0 KPH (35 mph)

Table 10: Description of Test 2

Test Number 40549-1	
Test Date:	October 19, 1995
Test Configuration:	Vehicle into 42-inch (1.07 m) vertical wall with 25 Degree Impact Angle
Vehicle:	Chevrolet C-2500 1989 Model Year
Engine Type	5.7 V8 transverse front mount
Transmission Type:	Automatic
Vehicle Speed:	100 KPH (62.5 mph)

SIMULATION OUTPUT

The simulations were performed on a Silicon Graphics Power-Challenge system shared memory, SMP super computer consisting of 16 processors. The SMP version of the LS-DYNA3D, version 936 was used. Table 11 shows a comparison of the computation time required between the detailed and reduced models.

Table 11: Computation time required for detailed and reduced models

Simulation	**Model**	**No. of CPU's**	**Computation Time**

Frontal impact to a rigid wall	Detailed	2	61 hrs. 40 min
Frontal impact to a rigid wall	Reduced	2	2 hrs 20 min.
Corner Impact to a vertical wall	Detailed	2	112 hrs 40 min.
Corner Impact to a vertical wall	Reduced	2	4 hrs. 30 min.

.In both simulation cases for the detailed model, a fixed time step of 1 microsecond was used. For the reduced model, a fixed time steps of 4 microseconds was used. In both the detailed and reduced models, the acceleration records for selected nodal points were outputted every 0.05 milliseconds. These nodal points were chosen based on the sensor locations of the test vehicles. For frontal impact with rigid wall, these positions include: engine, dash-board, and cabin rail while in the 42-inch Vertical Concrete Median the center of gravity (Cg) was added.. An SAE-60 filter was used to reduce numerical noise effects in the simulation for nodal acceleration records, as well as for the test data. The acceleration records are shown along with the test results in the next section.

COMPARISON OF TEST AND SIMULATION

The accuracy and fidelity of the simulations were studied in the following stages: 1) crash deformation profile in the high impact regions; 2) time history records at different locations; 3) energy absorption by different components; and 4) general motion of vehicle. Since the electronic data for the corner impact into the vertical concrete median is under study, stage 3 of the analysis is not yet complete for both detailed and reduced models

Frontal Impact with a Full Rigid Barrier

Detailed Model

Crash Deformation Profile in the High Impact Zone-The general deformation at the impact regions can be compared visually from the images captured with the high speed cameras. Figures 8 and 9 show the side and top view of the truck at the initial state and at 39 msec. The 39 msec state is selected because it represents the progression of the deformation on the hood and fenders. These figures also show the same views of the truck but at 60 msec and 90 msec. These states were selected because they represent the stage at which much of the plastic deformation has occurred. It can be observed from the figures that the deformation profiles in hood, fender, and bumper show good correlation between the simulation and the full scale test. Figure 10 shows the bottom view of the truck at the initial state, 39 msec, 60 msec and 90 msec

t = 0 msec t = 39 msec t = 60 msec t = 90 msec

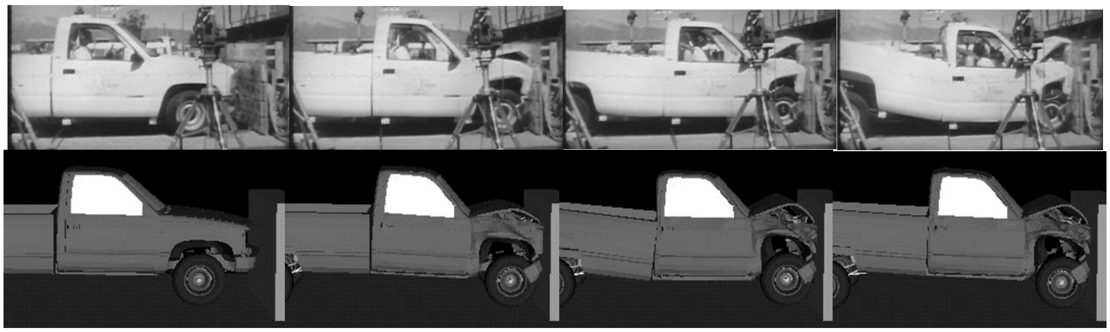

Figure 8: Side view of detailed model simulation and test for truck into rigid wall

t = 0 msec t = 39 msec t = 60 msec t = 90 msec

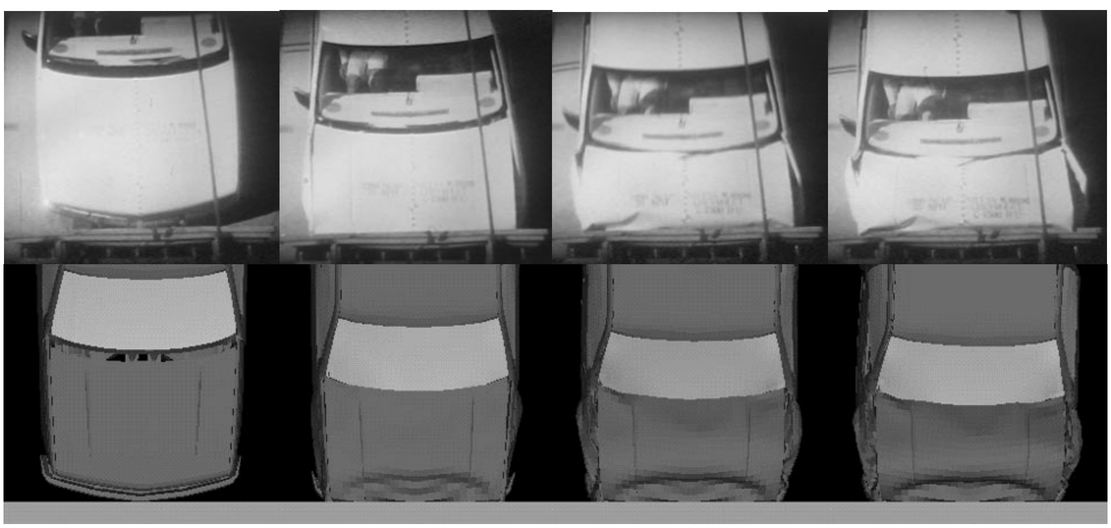

Figure 9: Top view of detailed model simulation and test for truck into rigid wall

t = 0 msec t = 39 msec t = 60 msec t = 90 msec

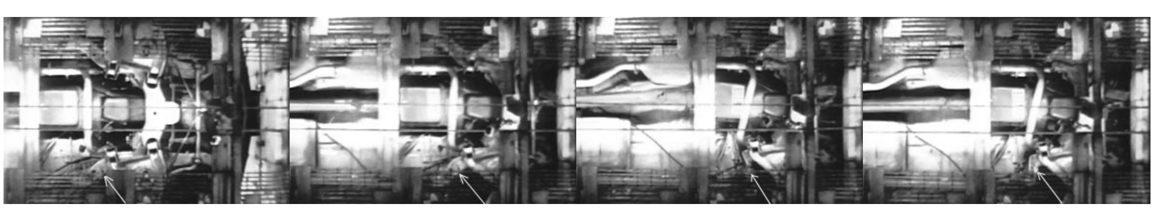

Figure 10: top view of detailed model simulation and test for truck into rigid wall

An arrow was added at the bottom of each image to emphasize the similarity in the plastic deformation of the rails. The general deformation occurring at the bottom of the truck shows a good correlation between simulation and test.

<u>Time History Records at Different Locations</u> - The next level of comparison is the velocity and acceleration time histories at the different locations. Figure 11a shows the comparison of the acceleration record between test and simulation. The accelerometers are located at the bottom of the engine, and on the rear right side of the bench seat. It can be observed that the curve shapes and peak values show good correlation and consistency. The maximum deceleration seen by the engine is 96 g's while that observed in the cabin is 52.3 g's. The errors in prediction are 3.3 % and 16.5 % respectively. Figure 11b is the comparison of velocity time histories of test and simulation taken from the rear left side of the bench seat and the top of the engine. The comparison shows a reasonable agreement between the test and simulation. However, the test is more compliant. This could be attributed to the material properties used in the model, thus emphasizing the importance of material testing and characterization. Variable time steps can be used to reduce simulation error by a factor of 3 [10], particularly in the high impact zone, at the expense of the computational time. For instance, when a variable time step was used, the CPU time for a frontal impact to a rigid wall simulation was 212 hours compared to 49 hours with a fixed time step of 1 microsecond.

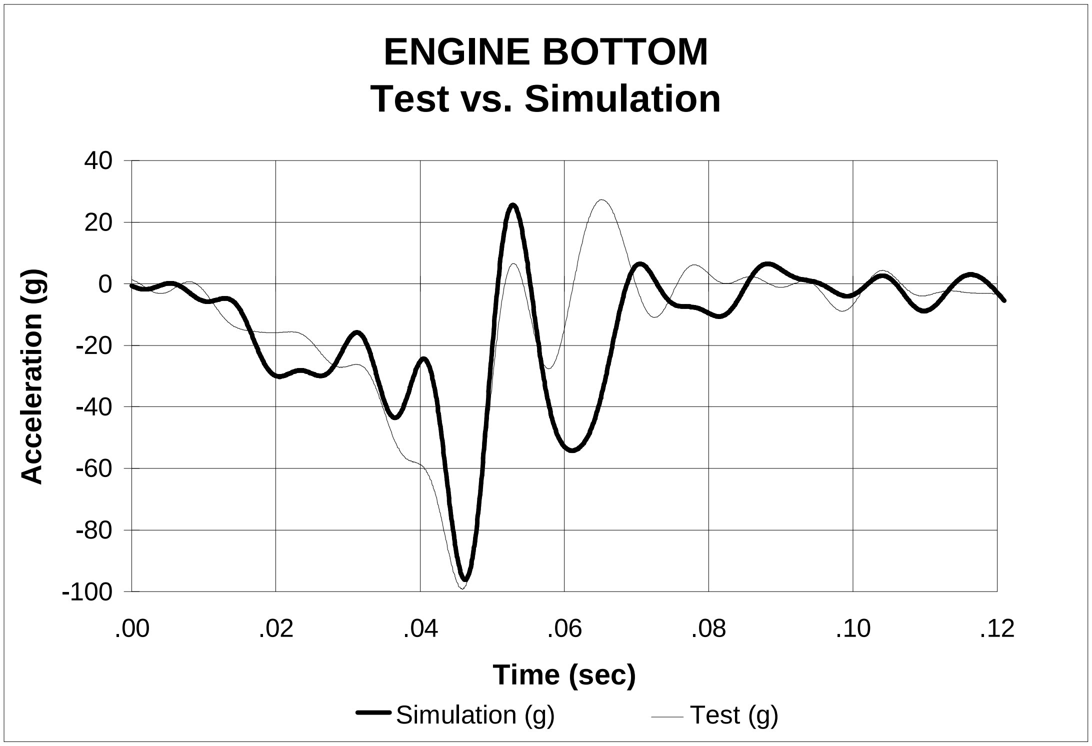

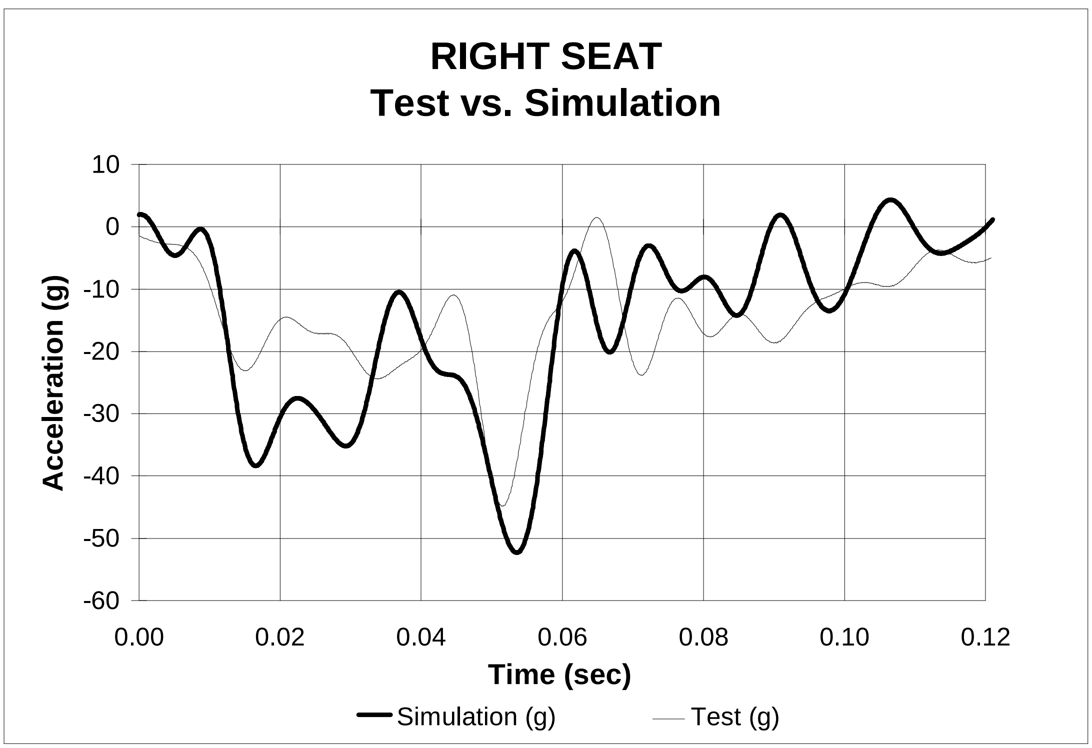

Figure 11a: Acceleration comparison for test and simulation for frontal impact into a rigid wall

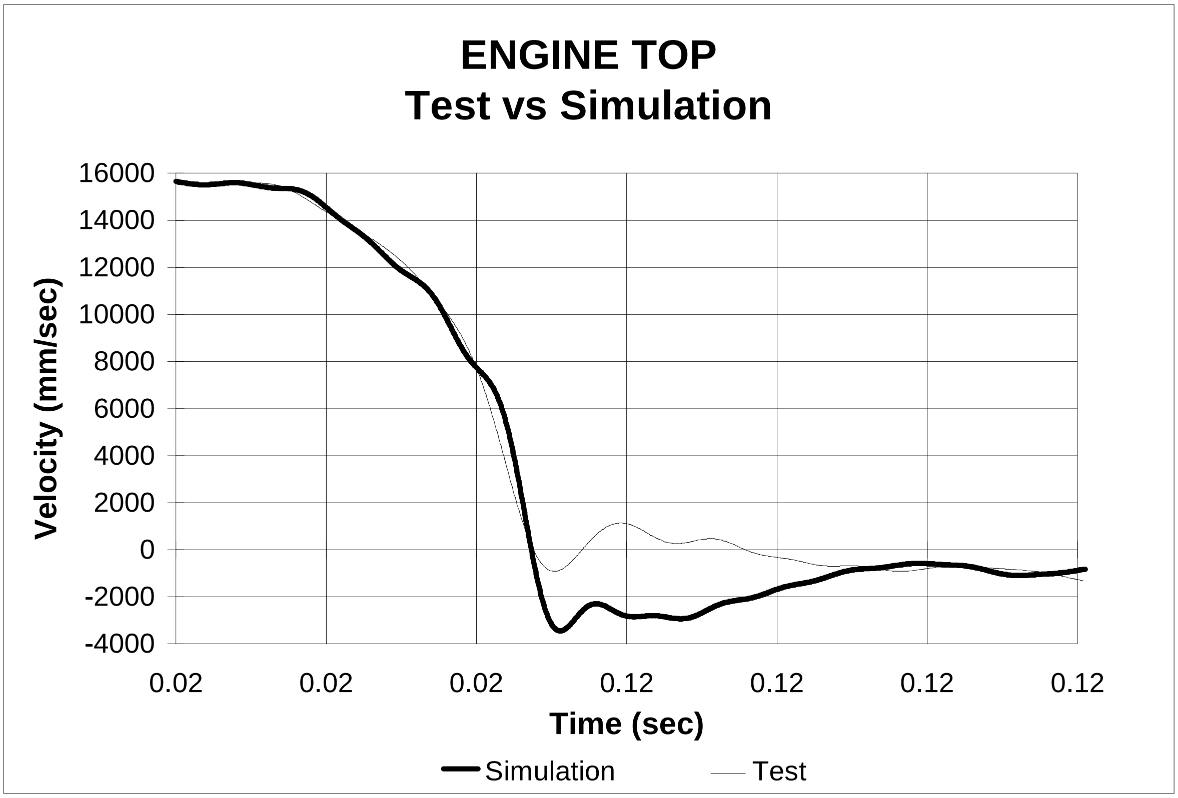

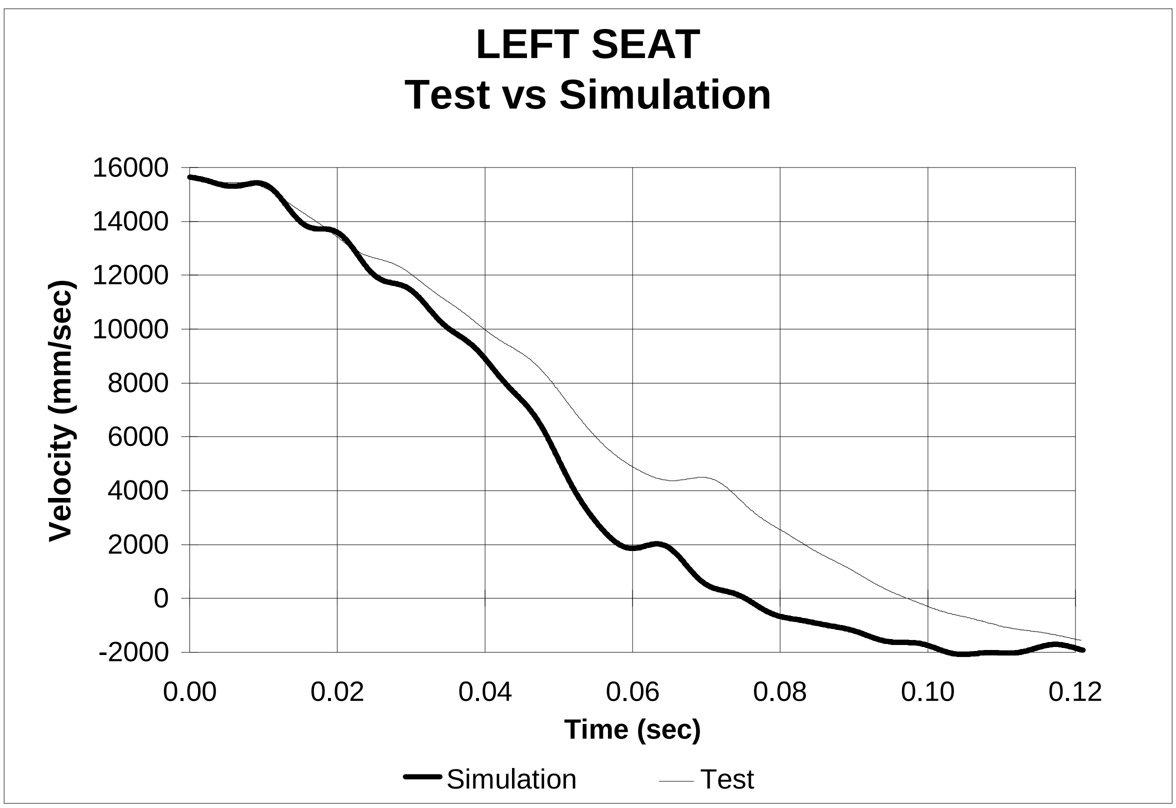

Figure 11b: Velocity comparison for test and simulation of frontal impact to a rigid wall

<u>Energy Absorption by Different Components</u> - It is important to analyze the energy absorption by the different components in the vehicle. This can be obtained in the simulation by computing the material internal energies in the model. The internal energy of the materials is the sum of the plastic strain energy and the elastic strain energy as shown in Figure 12. Table 12 shows the percent of total energy mitigated through the different components.

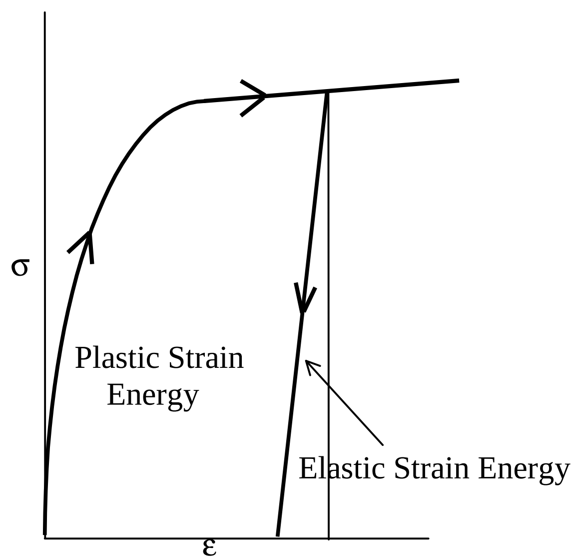

Figure 12: Plastic and elastic strain energies

Table 12: Material Internal Energy for a 35 mph Frontal Impact into a Rigid Wall

Material Parts	**Internal Energy (KJoules)**	**Percentage**
Whole Vehicle	214	100%
Rails and its matching structures	93.20	43.55%
Bumper and its matching structures	26.10	12.20%
Engine and its matching structures	23.00	10.75%
Radiator and its matching structures	21.80	10.19%
Toepan and front floor	15.20	7.10%
Hood	10.70	5.00%
Fender	9.80	4.58%
Wheelhouse	1.65	0.77%
Remaining components	12.50	5.84%

The total initial kinetic energy in the model can be computed using the following equation:

$$E = \frac{1}{2}mv^2 \qquad (1)$$

Where m represents the mass of the vehicle, and v the velocity. Applying equation 1 for the truck with $m = 1893.3$ Kg, and $v = 15.65$ m/s results in:

$$E = 231.86 \text{ KJoules}$$

The initial kinetic energy obtained from the simulation is 237 KJoules. The 2.5% difference between the initial kinetic energy computed manually using equation 1 (231.86 KJoules) and the one obtained from the simulation (237 KJoules) is primarily caused by round-off errors and increased mass resulting from using a larger time step than the one dictated by Courant's criteria. This is done to avoid the smallest elements in the model from controlling the time step. The accuracy of the model is not affected by this slight increase, but these elements incur a modest increase in mass such that the Courant criteria is satisfied.

Another important step in the energy balance analysis is to ensure that the conservation of energy condition is satisfied. This can be checked by comparing the final energy and initial energy in the model. The initial energy in this case is mainly attributed to the kinetic energy while the final energy is mainly attributed to internal energy. When comparing the initial kinetic energy and the final internal energy in the model, a difference of 23 KJoules is seen. This portion of energy is basically the kinetic energy left in final state (i.e. the truck impacts the wall and bounces back with a much smaller velocity causing a 23 KJoules of kinetic energy).

The data shown in Table 8 is also important in determining the importance of the respective components to the accuracy and fidelity of the model and the overall simulation. The percent of total energy absorption appears to be consistent with engineering intuition. The results show favorable energy distribution compared with some simulation results of the less detailed model [10].

General Motion of Vehicle -. Observation of the actual crash test of the frontal impact shows good correlation of movements of engine, transmission and drive shaft as shown in Figure 13 for the bottom view. It is noticed that the transmission moved upward in the pictures for both test and simulations emphasized by an arrow. The general similarities between test and simulation can also be noticed in figure 3 at t = 90 msec, where pitching of the flat bed occurs.

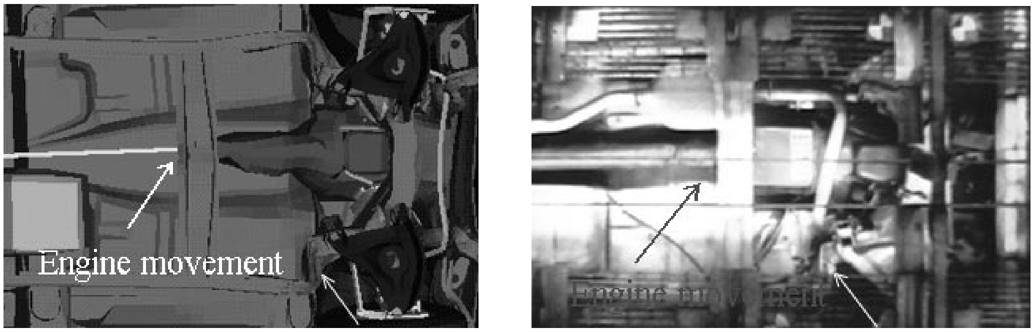

Figure 13: Bottom view of the frontal impact showing the engine movement

Reduced Model

<u>Crash Deformation Profile in the High Impact Zone</u>-Similar to the detailed model case, the general deformation at the impact regions can be compared visually from the images captured with the high speed cameras. Figures 14, 15 and 16 show the side, top and bottom view of the truck at the initial state, 39 msec., 60 msec. and at 90 msec. It can be observed from these figures that the deformation profiles in hood, fender, and bumper show reasonable correlation between the simulation and the full scale test. However, it is obvious that the reduced model lacks the necessary details in certain parts, specifically at the hood.

t = 0 msec t = 39 msec t = 60 msec t = 90 msec

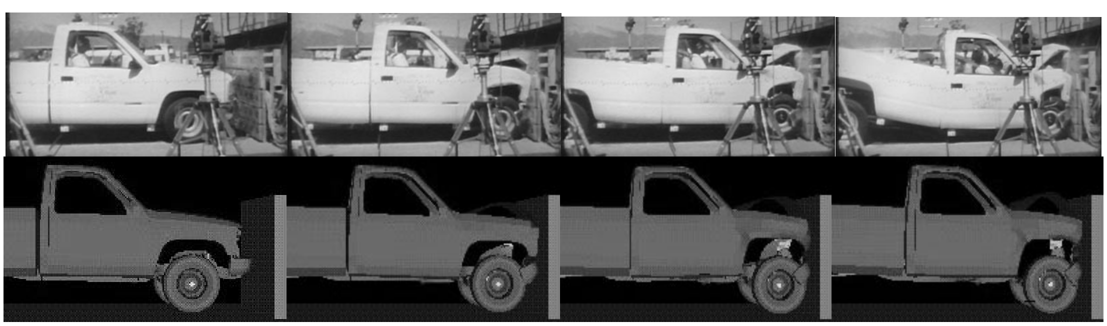

Figure 14: Side view of reduced model simulation and test for truck into rigid wall

t = 0 msec t = 39 msec t = 60 msec t = 90 msec

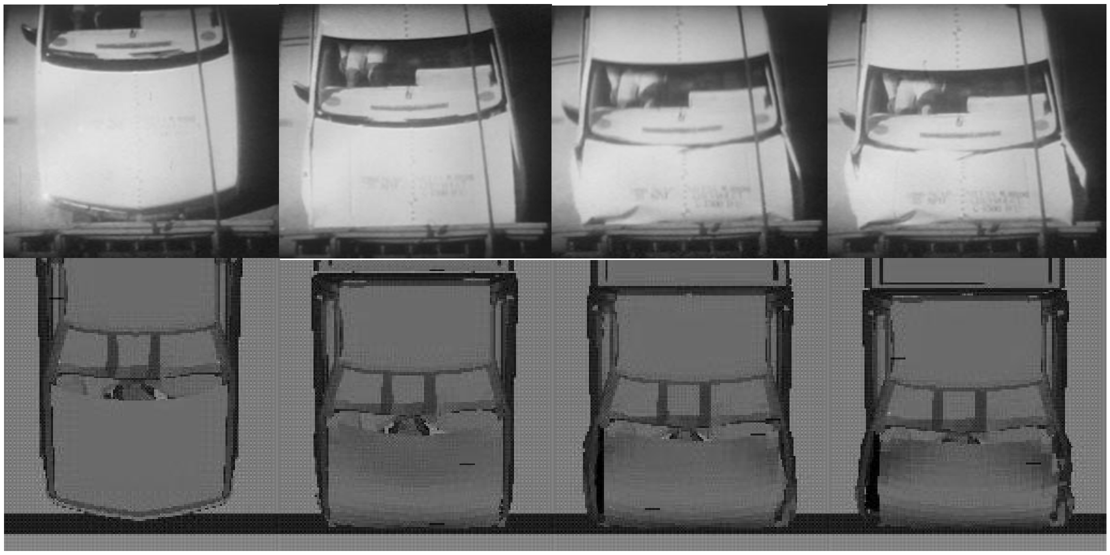

Figure 15: Top view of reduced model simulation and test for truck into rigid wall

t = 0 msec t = 39 msec t = 60 msec t = 90 msec

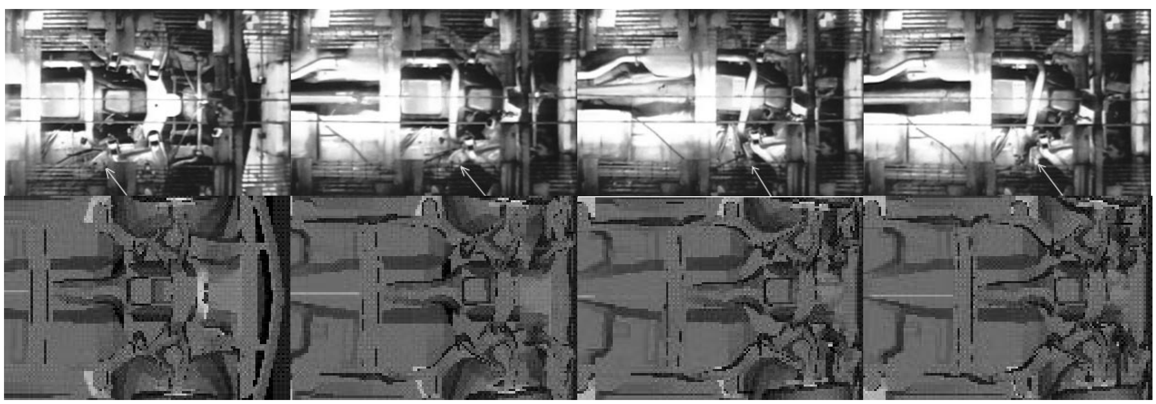

Figure 16: top view of reduced model simulation and test for truck into rigid wall

Time History Records at Different Locations - Figure 17a shows the comparison of the acceleration record between test and simulation. The accelerometers are located at the bottom of the engine, and on the rear right side of the bench seat. The maximum deceleration seen by the cabin is 45 g's. The error in prediction is 11 percent. However, the simulation curve is not in agreement with the test curve. This could be caused by the parts not included in the reduced model. Figure 17b is the comparison of velocity time histories of test and simulation taken from the bottom of the engine. The comparison shows a reasonable agreement between the test and simulation.

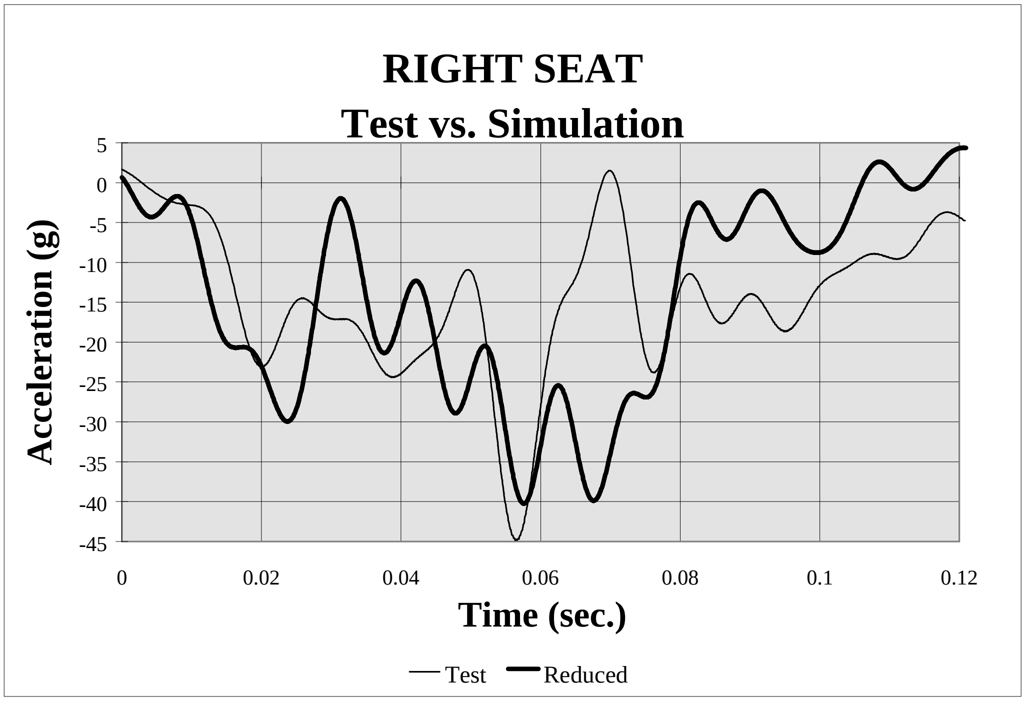

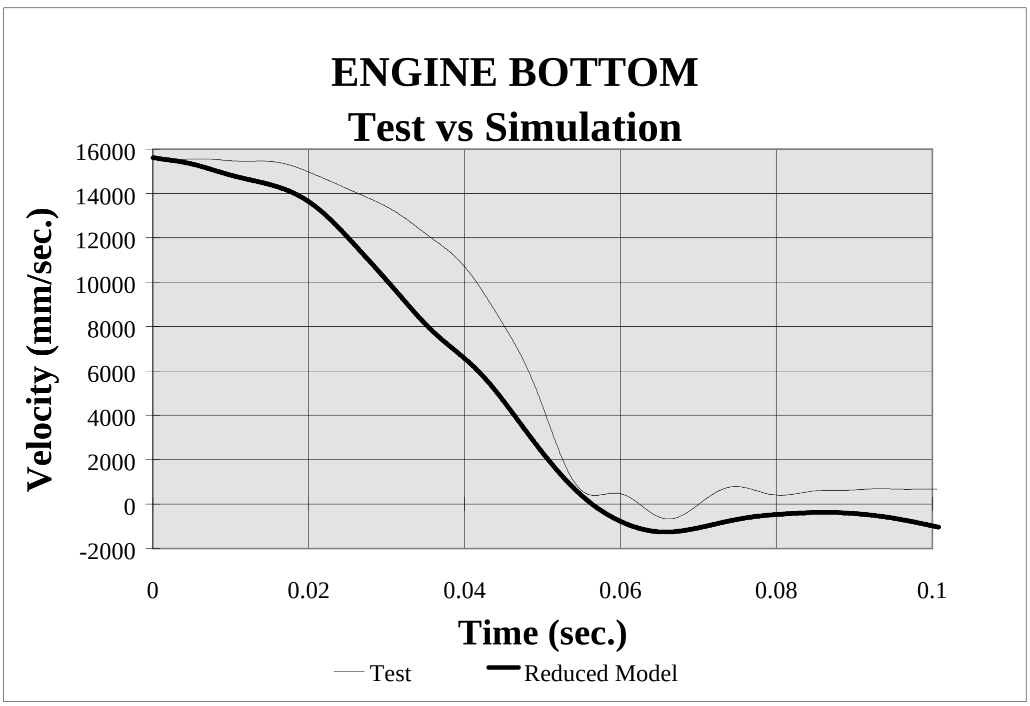

Figure 17: Acceleration and velocity comparison for test and simulation for frontal impact into a rigid wall

Energy Absorption by Different Components

Table 12 shows the percent of energy mitigated through the different components of the reduced model.

Table 13: Material Internal Energy for a 35 mph Frontal Impact into a Rigid Wall

Material Parts	Internal Energy (KJoules)	Percentage
Whole Vehicle	220	100%
Rails and its matching structures	100	45.50%
Bumper and its matching structures	53	24.00%
Fenders	18	8.20%
Radiator and its matching structures	15	6.80%
Hood	11	5.10%
Other	23	10.40%

The initial kinetic energy obtained from the simulation is 262 KJoules. There is a 17% difference between the kinetic energy dissipated during the impact and the internal energy absorbed by the truck.. This difference is caused by hourglassing attributed to the larger size of the elements used in the reduced model. Due to the severity of this type of impact, large deformations occur leading to more hourglassing then expected.

General Motion of Vehicle -. The general deformation of the reduced model shows reasonable correlation. Pitching of the flat bed can be seen, although not as apparent as in the detailed model case.

Corner impact into a 42-inch vertical concrete barrier

Detailed Model

Crash Deformation Profile in the High Impact Zone - The truck tested, C-2500, is a 5.7 Liter V8 with an automatic transmission. This configuration adds a total of 300 Kg to the gross vehicle weight, when compared to the C-1500 equipped with the 4.3 liter Vortec V6. Therefore, weight was added to the model at the engine, transmission, and rear axles. Figures 18 and 19 show the top and front view of the truck at the initial state and at 75 msec. The 75 msec state is selected because it represents the progression of the deformation. These figures also show the same view of the truck but at 120 msec and 240 msec. These states were selected because they represent the stages at which much of the plastic deformation has occurred. Good correlation can be observed from these figures between test and simulation, such as the door opening on the driver’s side and the cabin motion with respect to the bed.

t = 0 msec t = 75 msec t = 120 msec t = 240 msec

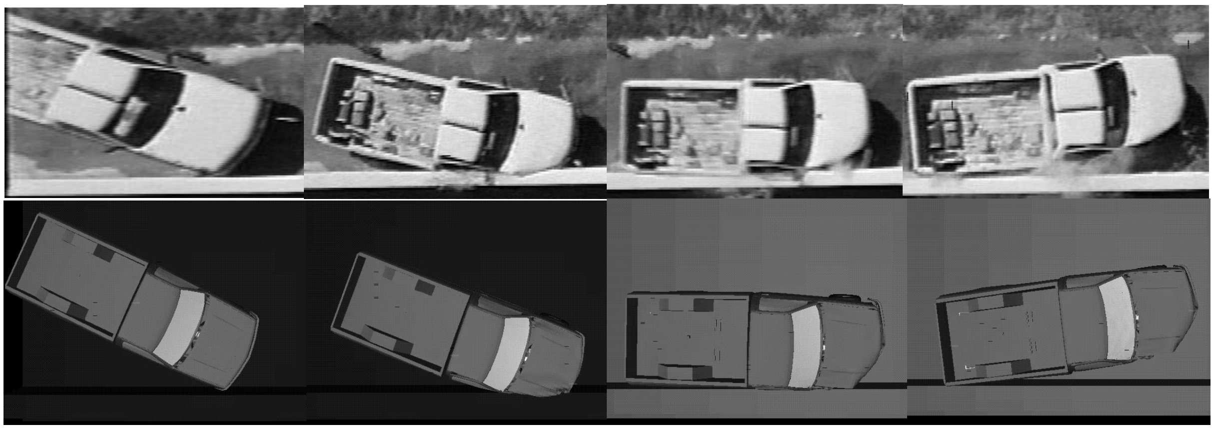

Figure 18:Top view of simulation and test for truck into 42-inch vertical barrier

t = 0 msec t = 75 msec t = 120 msec t = 240 msec

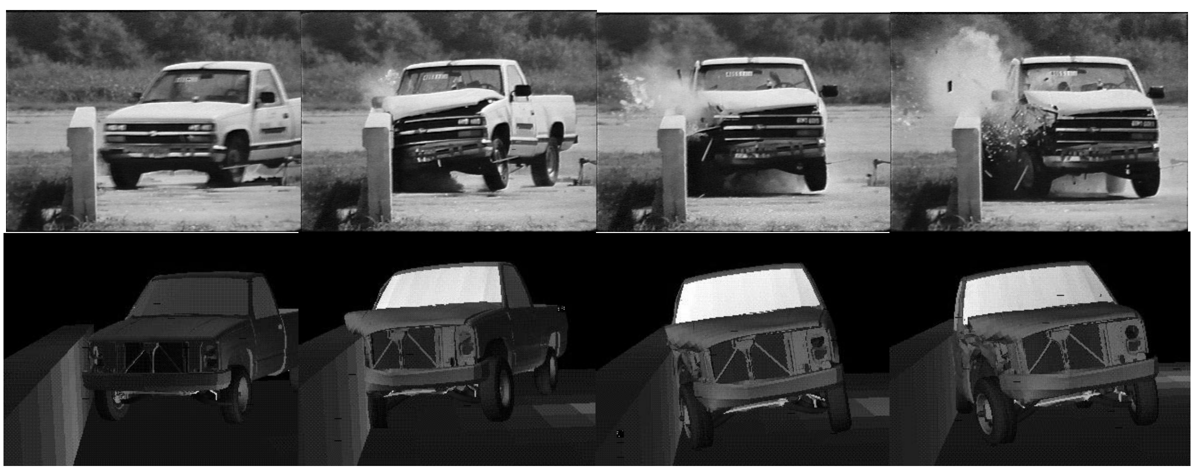

Figure 19: Front view of simulation and test for truck into 42-inch vertical barrier

<u>Time History Records at Different Locations</u> - For the next level of comparison, the velocity time history of test and simulation taken from the truck's center of gravity can be seen in Figure 20.

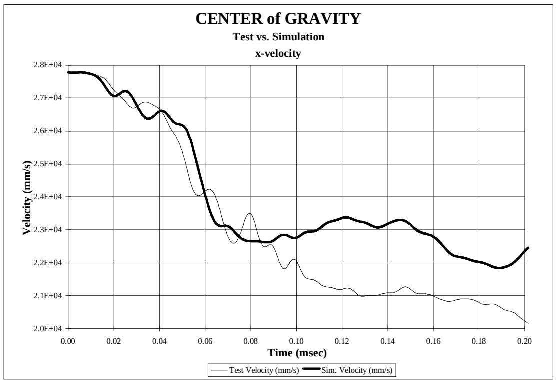

Figure 20: Velocity comparison for test and simulation for corner impact into a rigid barrier

The comparison shows reasonable agreement and, as in the previous case, the test seems to be more compliant. However, no accurate conclusion can be drawn since the data analysis is not complete.

Energy Absorption by Different Components - Table 14 shows the percent of total energy mitigated through the different components. It can be seen that the percent of energy absorption is more distributed than the frontal impact into a rigid wall. This is due to the nature of the impact which causes damage along a larger portion of the truck. The energy absorption appears to be consistent with engineering intuition and the results show good energy distribution.

Table 14: Material Internal Energy of detailed model for 62 mph Corner Impact into a Rigid Barrier

Material Parts	Internal Energy (KJoules)	Percentage
Whole Vehicle	147.75	100%
Wheels and tires	29.28	19.82%
Rails and its matching structures	26.78	18.13%
Engine and its matching structures	16.11	10.90%
Radiator and its matching structures	15.19	10.28%
Fender	10.06	6.81%
Hood	9.90	6.70%
Bed	9.50	6.33%
Front Suspension	8.65	5.85%
Bumper and its matching structures	8.40	5.69%
Wheelhouse	6.27	4.24%
Toepan and front floor	3.06	2.07%
Rear Suspension	3.00	2.03%
Door	1.70	1.15%

Similar to the full wall case, the initial kinetic energy for the 42 in. vertical concrete median case can be determined using equation 1. The mass of the truck model, however, is slightly higher in this case than that of the previous case (2002 kg as opposed to 1893.3 Kg). This difference in mass is mainly due to the difference in engine size and capacity (5.7L V8 as opposed to 4.3L V6). The initial velocity, 28.69 m/s, is also higher than the one used in the first case (15.65 m/s). Using equation 1, the initial kinetic energy is found to be 797.3 KJoules. This kinetic energy compares reasonably well to the one obtained from the simulation, 800.6 KJoules. The difference is attributed to approximations made in the manual computation of the initial kinetic energy. and increased mass resulting from using a larger time step than the one dictated by Courant's criteria, as discussed previously in the full wall case.

Since no external forces are applied to the system, the total energy in the model must be conserved. This can be verified by comparing the initial and final energies. The total initial energy of the system is equal to the initial kinetic energy (800.6 KJoules) since there are no deformations in the initial state. The total final energy in the sum of the final kinetic energy (650.3 KJoules) and the final internal energy (147.75 KJoules). Comparing the total initial and final energies, it can be concluded that energy in the system is conserved. \

General Motion of Vehicle - As mentioned previously, the validation process is not complete without the overall evaluation of the crash mechanics. Observation of the actual crash test of corner impact shows good correlation of post crash movement as shown in figures 8 and 9. The truck exhibits good rigid body motion; the images show the truck impacting, hugging and then leaving the barrier.

Reduced Model

Crash Deformation Profile in the High Impact Zone - Figures 21 and 22 show the top and front view of the truck at the initial state, 75 msec, 120 msec and 240 msec. These states were selected because they represent the stages at which much of the plastic deformation has occurred. Good correlation can be observed from these figures between test and simulation.

t = 0 msec t = 75 msec t = 120 msec t = 240 msec

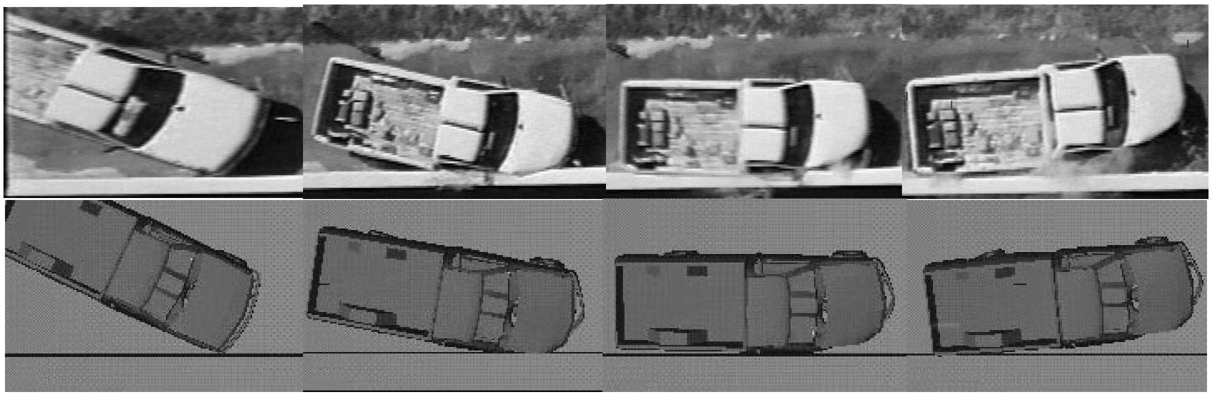

Figure 21: Top view of simulation and test for truck into 42-inch vertical barrier

t = 0 msec t = 75 msec t = 120 msec t = 240 msec

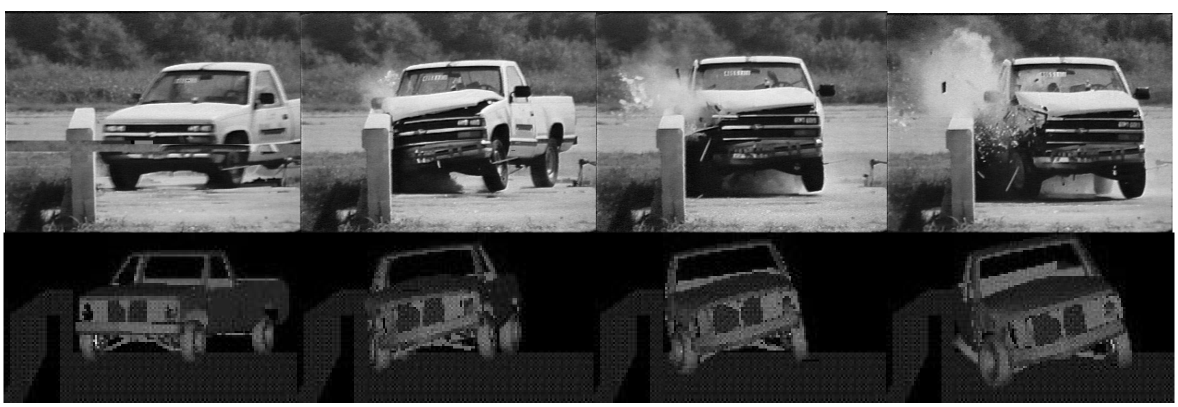

Figure 22: Front view of simulation and test for truck into 42-inch vertical barrier

<u>Time History Records at Different Locations</u> - Data for this level of evaluation was still under study at the time of this writing.

<u>Energy Absorption by Different Components</u> - Table 15 shows the percent of total energy mitigated through the different components. Similar to the detailed model, the energy absorption is distributed along a large region. This is attributed to the nature of the impact which causes damage along a large portion of the vehicle.

Table 15: Material Internal Energy for 62 mph Corner Impact into a Rigid Barrier

Material Parts	Internal Energy (KJoules)	Percentage
Whole Vehicle	91	100%
Rails and its matching structures	25.80	28.40%
Bumper	12.40	13.60%
Wheels and tires	11.00	12.00%
Radiator and its matching structures	10.80	11.90%
Fender	10.00	11.10%
Hood	6.00	6.60%
Other	15.00	16.40%

The initial kinetic energy of the truck is 835 KJoules and the final kinetic energy is 736 KJoules. The difference between the initial and the final kinetic energy (89 KJoules) matches the total internal energy absorbed by the truck. As compared to the previous simulation (35 mph impact to a full rigid barrier), the hourglass energy was significantly lower. This is expected since the impact is less sever and the deformation is of lesser magnitude.

General Motion of Vehicle - Observation of the actual crash test of corner impact shows good correlation. The truck exhibits good motion; the images show the truck impacting, hugging and then leaving the barrier.

CONCLUSIONS

The detailed model simulation results are consistent with the crash tests in terms of different levels of comparison. Some of the problems can be resolved by modeling more components in the cabin interior, including seats, dashboard assembly, and dummies. Furthermore, additional simulations need to be performed using the variable time step integration to separate numerical errors from modeling errors. The model can be further improved by exercising different impact configurations including side impact with the moving deformable barrier (MDB), offset head-on and angle impact with another vehicle, and impact into roadside narrow objects and barriers such as the vertical concrete wall and guardrail.

The simulation results of the reduced model presented in this paper demonstrate an initial step at learning how to develop smaller vehicle models that require less computation time. These results are preleminary and show an attempt in understanding these types of models. Further improvement are necessary for the reduced model. Additional simulations need to performed using different impact scenarios to further evaluate the model.

ACKNOWLEDGMENT

This research is performed under the contract from U. S. Department of Transportation (DTFH61-92-C-00128). The authors wish to thank Mr. Hansjoerg Schinke for his helpful discussions and assistance with the simulation.

REFERENCES

1. Zaouk, A., Bedewi N.E., Kan, C.D., Schinke, H., "Evaluation of a Multi-purpose Pick-up Truck model Using Full Scale Crash Data with Application to Highway Barrier Impacts," Presented at the 29th International Symposium on Automotive Technology and Automation, Florence, Italy, June, 1996.
2. Zaouk, A., Bedewi N.E., Kan, C.D., Marzougui, D., "Validation of a Non-Linear Finite Element Vehicle Model Using Multiple Impact Data," International Mechanical Engineering Congress and Exposition, November 17-22, 1996, Atlanta, GA.
3. Belytschko, Ted, "On Computational Methods for Crashworthiness," *Proceedings of the 7th International Conference on Vehicle Structural Mechanics*, SAE, Detroit, 1988, pp. 93-102.
4. Cofie, E. and Ray, M. "Simplified finite element vehicle model," *Transportation Research Board Publications, Circular on Computer Simulation,* April, 1994.
5. Varadappa, S., Shyo, S. C., and Mani, A., "Development of Passenger Vehicle Finite Element Model," *Final Report DOT HS 808 145, Department of Transportation,* November 1993, Washington, DC.
6. Perfect, S. and Logan, R. "Evaluation of the Honda Civic Based FE Model," *Transportation Research Board Publications, Circular on Computer Simulation,* April, 1994.
7. Eskandarian, A., Bedewi, N.E., and Meczkowski, L., "FHWA/NHTSA National Crash Analysis Center," *Public Roads, A Journal of Highway research and Development,* US DOT, FHWA Office of R&D, 1993.
8. Eskandarian, A., Bedewi, N.E., and Meczkowski, L., "Finite Element Modeling of 4 Lb/Ft. U-Channel Post Sign Support Systems," *Research and Technology Transporter, a DOT, FHWA Quarterly Accomplishment Report.*

9. Eskandarian, A., Bedewi, N.E., and Marzougui, D., “Finite Element Impact Modeling of Highway Narrow Objects,” *Presented at the Transportation Research Board Annual Meeting/Conference, Session on Computer Simulation of Impacts with Roadside Safety Features*, Washington, DC, January 10-14, 1994.
10. Bedewi, N.E., Omar, T., and Eskandarian, A., “Effect of Mesh Density Variation in Vehicle Crashworthiness Finite Element Modeling,” *Proceedings of the ASME Winter Annual Meeting, Transportation Systems Session*, November 6-11, 1994, Chicago, Ill.
11. Kan, C. D. and Yang, C. “Impact of the Ford Taurus Based FE Model into a Rigid Pole,” *FHWA/NHTSA National Crash Analysis Internal Report.*, August 1994.
12. Bedewi, N.E., Kan, C.D., Summers, S., and Ragland, C., “Evaluation of Car-to-Car Frontal Offset Impact Finite Element Models Using Full Scale Crash Data,” Issues in Automotive safety Technology, SAE Publication SP-1072, pp 212-219, February, 1995.
13. Miller, L., Bedewi, N., and Chu, R., “Performance Benchmarking of LS-DYNA3D for Vehicle Impact Simulation on the Silicon Graphics POWER CHALLENGE” *Presented at the High Performance Computing Asia 95*, Taiwan, October, 1995
14. Schinke, H., Zaouk, A., and Kan, C.D., “Vehicle Finite Element Development of A Chevy C-1500 Truck with Varying Application,” *FHWA/NHTSA National Crash Analysis Internal Report.*, May, 1995
15. *P3/PATRAN USER Manual*, PDA Engineering, Publication 903000, 1993.
16. Hallquist, J.O., *LS-DYNA3D Theoretical Manual*, Livermore Software Technology Corporation, LSTC Report 1018, 1991.
17. Hallquist, J.O., Stillman, D.W., Lin, T.L., *LS-DYNA3D Users Manual* Livermore Software Technology Corporation, LSTC Report 1007, Rev. 2, 1992.
18. Schinke, H.,”HPD, A PATRAN to DYNA Translator,” *FHWA/NHTSA National Crash Analysis Internal Report.*, April, 1995
19. Hallquist, J.O., Stillman, D.W., Lin, T.L., *LS-INGRID Userís Manual*, Livermore Software Technology Corporation, LSTC Report 1008 Rev. 2, 1992.